Large-Chern-Number Quantum Anomalous Hall Effect in Thin-Film Topological Crystalline Insulators

Chen Fang,[1,2,4] Matthew J. Gilbert,[3,4] and B Andrei Bernevig[2]
[1]Department of Physics, University of Illinois, Urbana, Illinois 61801-3080, USA
[2]Department of Physics, Princeton University, Princeton, New Jersey 08544, USA
[3]Department of Electrical and Computer Engineering, University of Illinois, Urbana, IIllinois 61801, USA
[4]Micro and Nanotechnology Laboratory, University of Illinois, Urbana, Illinois 61801, USA
(Received 27 June 2013; published 27 January 2014)

We theoretically predict that thin-film topological crystalline insulators can host various quantum anomalous Hall phases when doped by ferromagnetically ordered dopants. Any Chern number between ± 4 can, in principle, be reached as a result of the interplay between (a) the induced Zeeman field, depending on the magnetic doping concentration, (b) the structural distortion, either intrinsic or induced by a piezoelectric material through the proximity effect, and (c) the thickness of the thin film. We propose a heterostructure to realize quantum anomalous Hall phases with Chern numbers that can be tuned by electric fields.

DOI: 10.1103/PhysRevLett.112.046801 PACS numbers: 73.43.-f, 72.20.-i, 73.20.At

A quantum anomalous Hall state is a 2D topological insulating state that has quantized Hall conductance in the form of Ce^2/h, where C is an integer, and possesses $|C|$ gapless edge modes along any 1D edge. These properties are shared by the well-known quantum Hall states [1]. Nevertheless, there is no external magnetic field in a QAH state, which makes it "anomalous." Hence, the nontrivial topology in QAH does not come from the topology of the Landau levels, but rises from the band structure of electrons coherently coupled to certain magnetic orders, e.g., spin orders and orbital current orders. The first theoretical model that shows this phase is given in Ref. [2], which is followed by other models and experimental proposals in various systems [3–8]. Very recently, experimentalists have adapted one of the proposals and realized a QAH state with $|C| = 1$ in chromium doped thin-film $(\mathrm{Bi,Sb})_2\mathrm{Te}_3$, which is a 3D topological insulator (TI) [9,10].

We first recapitulate the basic idea underlying the realization of QAH insulators with $|C| = 1$ in a thin-film 3D topological insulator[4–7]. Each surface of a 3D TI is a gapless 2D Dirac spin-split semimetal [11,12], as opposed to spin-degenerate Dirac semimetals such as graphene. The surface is spin split except at the Dirac point where double degeneracy is protected by time-reversal symmetry, and spectral flow into the bulk conduction and valence bands occurs away from the Dirac point. Upon the application of a Zeeman field along the perpendicular direction, induced by ferromagnetic dopants, a gap is opened at the Dirac point, giving rise to a massive Dirac cone. Such a massive Dirac cone has been well known to contribute Hall conductance of $\pm e^2/2h$ [4,13], or, a Chern number of $\pm 1/2$. Moreover, since a thin film has two surfaces (top and bottom), the total Chern number is ± 1. An identical effect would take place in bulk samples—thin films are being used here only because they allow tuning of the Fermi level in the gap by gating [14,15]. Here we use a symmetry-based analysis to show that the topological crystalline insulators [16–24] [such as (Pb,Sn)(Te,Se)] are much richer compounds to explore QAH physics. As thin films of (Pb,Sn)(Te,Se) have already been grown [25–27] and various magnetic dopants have been successfully doped [28–30], we believe our proposal is experimentally realizable. The existence of such a widely tunable topological phase transition in the topological crystalline insulator (TCI) class of materials may form the basis for new types of information processing devices which consume much less power compared to current technology.

Consider the symmetries of such a thin film. (Pb,Sn)(Te,Se) crystalizes into a face-centered-cubic lattice with point group O_h. Below a critical temperature, depending on composition, the cubic symmetry spontaneously breaks into either rhombohedral or orthorhombic symmetries, resulting in a small lattice distortion. Here we assume that the lattice has cubic symmetry and treat the small distortion as a perturbative strain. The thin-film sample is terminated on the (001) plane, where O_h reduces to a 2D point group C_{4v}. The bulk system also has time-reversal symmetry and inversion symmetry, which relates the top and the bottom surfaces in the absence of asymmetric surface terminations. The in-plane translational symmetry allows the definition of the surface Brillouin zone, which is centered at $\bar{\Gamma}$ and bounded by $\bar{X}$ along the [110] direction and $\bar{Y}$ along the $[1\bar{1}0]$ direction [Fig. 1(a)]. Four Dirac points close to the Fermi energy have been observed in experiments [18–20]. Two Dirac points, denoted by $D_{1,2}$, are located along $\bar{\Gamma}\bar{X}$, close to and symmetric about $\bar{X}\bar{M}$; two others, denoted by $D_{1',2'}$, are located along $\bar{\Gamma}\bar{Y}$, close to and symmetric about $\bar{Y}\bar{M}$. The band dispersion around any of the four Dirac

 © 2014 American Physical Society

points is linear in all directions to first order, resulting in four copies of a spin-split Dirac semimetal, related to each other by 90° rotations [Fig. 1(b)]. Recently, scanning tunneling spectroscopy measurements suggest [24] that in the rhombohedral phase, two of the four Dirac points are gapped [Fig. 1(c)].

We assume that the Fermi level is exactly at the Dirac point energy. While this is not true in bulk samples due to intrinsic impurity doping, in thin-film samples the Fermi level can be tuned anywhere in the bulk gap. Since the change in the Chern number only depends on the electronic states near the gap-closing points, i.e., the four Dirac points, we start by deriving the effective theories for each Dirac cone and then consider their coupling to gap-opening perturbations. The minimal model for each Dirac cone $h_{i=1,2,1',2'}(\mathbf{q})$, where $\mathbf{q} = \mathbf{k} - \mathbf{D}_i$, is a two-band $\mathbf{k}\cdot\mathbf{p}$ model, due to the double degeneracy at D_i. The form of h_i is determined by how the doublet at D_i transforms under the little group at D_i, i.e., a subgroup of the full symmetry group which leaves D_i invariant. For example, consider D_1: the little group is generated by the mirror reflection about the $(1\bar{1}0)$ plane, denoted by $M_{1\bar{1}0}$ and a combined operation of a 180° rotation about the [001] direction followed by time reversal, denoted by C_{2T}. This little group has only one 2D irreducible representation [31]: $M_{1\bar{1}0} = i\sigma_y$ and $C_{2T} = K\sigma_x$, where K means complex conjugation, and $\sigma_{x,y,z}$ are Pauli matrices. It restricts $h_1(\mathbf{q})$ to the form

$$h_1(\mathbf{q}) = v_0 q_1 I_{2\times 2} + v_1 q_1 \sigma_y + v_2 q_2 \sigma_x \quad (1)$$

up to the first order of $|q|$. $\mathbf{q}$ decomposes into two components $q_1 = \mathbf{q}\cdot\hat{e}_{110}$ and $q_2 = \mathbf{q}\cdot\hat{e}_{1\bar{1}0}$, where $\hat{e}_{mnl}$ is the unit vector along the $[mnl]$ direction. The parameters $v_{0,1,2}$ can be fixed by matching the dispersion of Eq. (1), $E(\mathbf{q}) = v_0 q_1 \pm \sqrt{v_1^2 q_1^2 + v_2^2 q_2^2}$ to the measured Fermi velocities along the [110] and $[1\bar{1}0]$ directions $[(v_0, |v_1|, |v_2|) \sim (0, 1.1, 2.8)$ ev Å]. The Dirac cones centered at $D_{2,1',2'}$ can be related to the cone centered at D_1 by C_4 symmetry. This automatically gives the effective theories of the other Dirac cones: $h_2(q_1, q_2) = h_1(-q_1, -q_2)$, $h_{1'}(q_1, q_2) = h_1(-q_2, q_1)$ and $h_{2'}(q_1, q_2) = h_1(q_2, -q_1)$[31].

We assume a Zeeman field in the sample along the [001] direction, induced by ferromagnetically ordered dopants. In order to couple this field to the electrons in the $\mathbf{k}\cdot\mathbf{p}$ models, we add an additional term δH_i^Z to $h_{i=1,2,1',2'}(\mathbf{q})$ and note the following facts: (i) magnetization along the [001] direction changes sign under both $M_{1\bar{1}0}$ and C_{2T} and (ii) it is invariant under 90° rotations about the [001] direction. Using these facts, we have,

$$\delta H_i^Z \equiv \delta H^Z = \Delta_Z \sigma_z + O(|q|),$$

where $|\Delta_Z|$ is the field strength of the Zeeman field, which is proportional to the Curie temperature, T_c, of the ferromagnetism. The sign of Δ_Z depends on the direction of the magnetization. The Hamiltonian for each cone with the induced Zeeman field is $h_i(\mathbf{q}) + \delta H^Z$, which has a gap of size $|\Delta_Z|$ at each Dirac point [see Fig. 2(b)].

Now we consider the effect of intrinsic and external strains. Depending on the Sn and Se concentration, the cubic lattice can have spontaneous distortions into either rhombohedral or the rhombohedral symmetries. One may also cap the top surface of the film with a piezoelectric material such as $BaTiO_3$, to control the strain on the top surface. A general strain tensor is given by a symmetric matrix ϵ_{ij}, where $i,j = 1, 2, 3$ written in the frame spanned by $(\hat{e}_{110}, \hat{e}_{1\bar{1}0}, \hat{e}_{001})$. In order to represent couplings to the strain tensor in the $\mathbf{k}\cdot\mathbf{p}$ models, we need to determine the transform of each component under the symmetry group C_{4v} and time reversal (Table I). Using these relations, we obtain the following strain induced terms for the four Dirac cones, to the zeroth order of $|q|$:

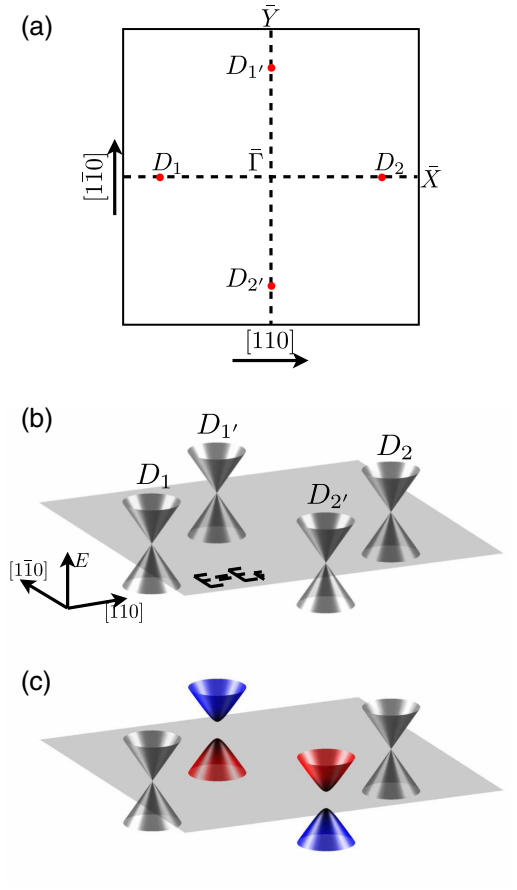

FIG. 1 (color online). (a) The surface Brillouin zone centered at $\bar{\Gamma}$ and bounded by $\bar{X}$, $\bar{Y}$, which is symmetric under 90° rotations about the vertical line through the center, and mirror reflections about the two dotted lines. The positions of the Dirac points are marked. (b) The schematics of the dispersion of the four Dirac cones on the (001) plane in the surface Brillouin zone. The middle plane is the $E = E_F$ plane passing through the four Dirac points at exact half filling. (c) The proposed surface dispersion of the rhomboderal phase with two massive and two massless Dirac cones, where a red (blue) cone contributes a fractional Chern number of $+1/2$ $((-1/2))$, respectively.

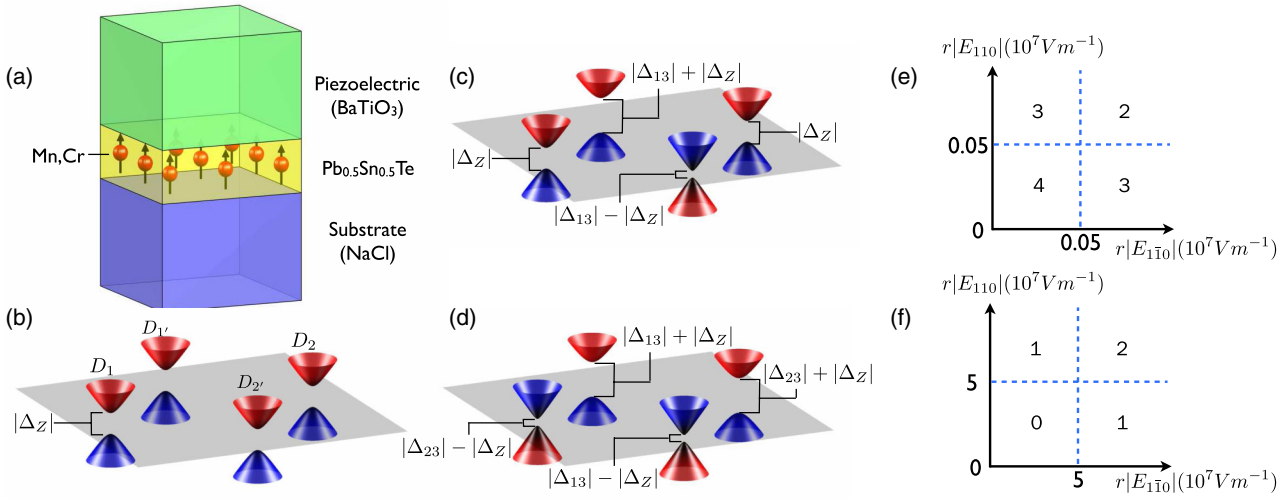

FIG. 2 (color online). (a) The schematic of a thin-film $Pb_{0.5}Sn_{0.5}Te$ grown on a substrate, capped by a piezoelectric. (b)–(d) The schematic dispersions of the gapped Dirac cones on the top surface in the presence of uniform Zeeman field and strains, corresponding to the parameters $\Delta_Z > |\Delta_{13}| = |\Delta_{23}| = 0$, $|\Delta_{13}| > \Delta_Z > |\Delta_{23}| = 0$, and $0 < \Delta_Z < |\Delta_{13}| = |\Delta_{23}|$, respectively. (e) The Chern number of the proposed system in the thick limit (sample thickness > 20 nm) plotted against the transverse electric fields applied on the piezoelectric. (f) The Chern number of the system with thickness of $5 \sim 10$ nm. Factor r in the front of the electric fields is the proportion of the strain that is transferred from piezoelectric to the sample.

$$\delta H^S_{1/2} = (\lambda_{11}\epsilon_{11} + \lambda_{22}\epsilon_{22} + \lambda_{33}\epsilon_{33} \pm \lambda_{13}\epsilon_{13})\sigma_y + \lambda_{12}\epsilon_{12}\sigma_x \pm \lambda_{23}\epsilon_{23}\sigma_z,$$

$$\delta H^S_{1'/2'} = (\lambda_{11}\epsilon_{22} + \lambda_{22}\epsilon_{11} + \lambda_{33}\epsilon_{33} \pm \lambda_{13}\epsilon_{23})\sigma_y - \lambda_{12}\epsilon_{12}\sigma_x \pm \lambda_{23}\epsilon_{13}\sigma_z,$$

where λ_{ij} are electrophonon couplings.

Consider the full Hamiltonian for each Dirac cone under both Zeeman field and strain, $H_i = h_i + \delta H^Z_i + \delta H^S_i$. In H_i, only terms proportional to σ_z open gaps in the spectrum while others move the position of the Dirac point D_i. The gap at each D_i, i.e., the coefficient before the σ_z term in the Hamiltonians, denoted below by Δ_i, is

TABLE I. The first four rows show the transformation properties of each tensor component under the symmetry group $C_{4v} \otimes T$, where $\pm$ means invariant or inverted. The last four rows show which Pauli matrix is coupled to each component, to the zeroth order, in the effective theory for each Dirac cone.

	ϵ_{11}	ϵ_{22}	ϵ_{33}	ϵ_{12}	ϵ_{13}	ϵ_{23}
C_{2T}	+	+	+	+	−	−
$M_{1\bar{1}0}$	+	+	+	−	+	−
M_{110}	+	+	+	−	−	+
C_4	ϵ_{22}	ϵ_{11}	+	−	ϵ_{23}	$-\epsilon_{13}$
δH^S_1	σ_y	σ_y	σ_y	σ_x	σ_y	σ_z
δH^S_2	σ_y	σ_y	σ_y	σ_x	$-\sigma_y$	$-\sigma_z$
$\delta H^S_{1'}$	σ_y	σ_y	σ_y	$-\sigma_x$	σ_z	σ_y
$\delta H^S_{2'}$	σ_y	σ_y	σ_y	$-\sigma_x$	$-\sigma_z$	$-\sigma_y$

$$\Delta_{1,2} = \Delta_Z \pm \Delta_{23}, \qquad \Delta_{1',2'} = \Delta_Z \pm \Delta_{13},$$

where we have defined $\Delta_{13/23} \equiv \lambda_{23/13}\epsilon_{23/13}$. Each gapped Dirac cone contributes

$$\sigma^H_i = -\mathrm{sgn}(v_1 v_2 \Delta_i) e^2/(2h) \tag{2}$$

to the Hall conductance [31].

We have so far assumed that the top and the bottom surfaces are isolated from each other, and hence the total Hall conductance is

$$\sigma^H = \sum_{i=1,2,1',2'} \sigma^{H,t}_i + \sigma^{H,b}_i, \tag{3}$$

where superscript $t(b)$ denotes the top (bottom) surface. When the thickness is comparable to the decay length of the surface states, the hybridization gap between the two surfaces, denoted by Δ_H, becomes significant, and the total Hall conductance is generically not given by Eq. (3). Diagonalizing each $\mathbf{k}\cdot\mathbf{p}$ Hamiltonian with hybridization [31]

$$\tilde{H}_i = \begin{pmatrix} H^t_i & \Delta_H I_{2\times 2} \\ \Delta_H I_{2\times 2} & H^b_i \end{pmatrix}, \tag{4}$$

we have two scenarios. (i) If $\mathrm{sgn}(\Delta^t_i) = \mathrm{sgn}(\Delta^b_i)$ [where $\Delta^{t(b)}$ denotes the gap at top (bottom) surface], as Δ_H increases, the gap at D_i closes at $|\Delta_H| = \Delta_{i,Hc} \equiv \sqrt{|\Delta^t_i \Delta^b_i|}$ and reverses [see Fig. 3], and at $|\Delta_H| > \Delta_{i,Hc}$, the total contribution to σ^H vanishes; (ii) if $\mathrm{sgn}(\Delta^t_i) = -\mathrm{sgn}(\Delta^b_i)$, there is no quantum phase transition as Δ_H increases, and the total contribution to Hall conductance stays at zero. The complete expression for the Hall conductance is, therefore,

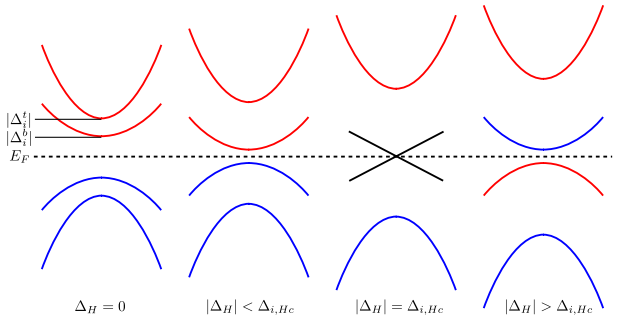

FIG. 3 (color online). The figures show the quantum phase transition happening at the Dirac cone centered at D_i which is induced by increasing the hybridization gap, Δ_H, between the top and the bottom surfaces. Here we start from a cone with $\Delta_i^t > \Delta_i^b > 0$ at $\Delta_H = 0$. Red (blue) means the represented cone contributes $\pm 1/2$ to the Chern number, respectively.

$$\sigma^H = \sum_{i=1,2,1',2'} (\sigma_i^{H,t} + \sigma_i^{H,b})\theta(\Delta_{i,Hc} - |\Delta_H|), \qquad (5)$$

where $\theta(x)$ is the Heaviside step function.

Depending on the parameter set of $\{\Delta_Z, \Delta_{13,23}^{t(b)}, \Delta_H\}$, the Chern number of the system takes each integer from -4 to $+4$. In a realistic system, however, not all parameters are easily tunable, so the range of the Chern number is generically restricted. We propose a system shown in Fig. 2(a): a thin-film $Pb_{0.5}Sn_{0.5}Te$ doped with Mn or Cr, epitaxially grown on a substrate, e.g., NaCl or KCl [32,33], with its top surface deposited or glued [34] with piezoelectric crystals such as $BaTiO_3$. Below $T \sim 10$ K, the (Cr, Mn) moments develop ferromagnetism, inducing a small Zeeman gap $\Delta_Z \sim 1$ meV in the sample [28]. The external strain on the top surface may be tuned by the piezoelectric. Assuming that the strain in $BaTiO_3$ be completely transferred to the top surface of the film, we estimate that [35–37] the $|\Delta_{13}^t| = 2 \times 10^{-6} E_{1\bar{1}0}\,\mathrm{meV\,m\,t\,V^{-1}}$ and $|\Delta_{23}^t| = 2 \times 10^{-6} E_{110}\,\mathrm{meV\,m\,V^{-1}}$. Practically, depending on the interface, only a certain proportion of the piezoelectric strain can be transferred, say $r < 1$, and the induced gaps should be multiplied by r. Since the sample with such composition has zero or negligible intrinsic distortion at low temperatures, $\Delta_{13,23}^b = 0$. In the thick limit ($d > 20$ nm), $\Delta_H \ll 1$ meV and is negligible [38]. [Also see Ref. [22], where a simulation of 33-layer thick sample (20 nm) shows negligible hybridization gap.] From Eq. (2), the bottom surface always contributes $C = 2$. There are three possible scenarios for the top surface, resulting in $\sigma^{H,t} = 2, 1, 0$, respectively, (i) $|\Delta_{13,23}^t| < |\Delta_Z|$, (ii) $|\Delta_{23}^t| < |\Delta_Z| < |\Delta_{13}^t|$, and (iii) $|\Delta_Z| < |\Delta_{13,23}^t|$, where we have assumed $|\Delta_{13}^t| > \Delta_{23}^t|$ without loss of generality. The dispersion of the four gapped cones for the three scenarios are plotted in Figs. 2(b)–(d). The total Chern number can thus be tuned between 2, 3, and 4, plotted against $E_{1\bar{1}0}$ and E_{110} in Fig. 2(e). In a thinner film with thickness $d = 5 \sim 10$ nm, the hybridization gap is $|\Delta_H| = 5 \sim 15$ meV [39], from which we take $\Delta_H = 10$ meV as a typical value and we plot the Chern number against $E_{1\bar{1}0}$ and E_{110} in Fig. 2(f). We see that around the critical field strength $|E_{1\bar{1}0}| = |E_{110}| = 5 \times 10^7\ \mathrm{V\,m^{-1}}/r$, the Chern number can be electrically tuned to 0, 1, or 2. If the length and width of the sample are both 100 nm, this means that the Chern number can be tuned by varying $V_{1\bar{1}0,110}$ within 10 mV. The ability to tune the topological phase transition with such a small electric field offers hope that such logic devices based on piezoelectric deformation of a TCI could possess on-to-off ratios and subthreshold slopes which far exceed current logic device technologies.

In the derivation of the main results, we have ignored physical factors of (i) the impurities and (ii) the electron-electron interaction. The mirror Chern number of a TCI is only well defined in the presence of mirror planes. In a system with a random impurity configuration, mirror symmetries are broken and the mirror Chern number is not a good quantum number, and, consistently, the gapless modes at the Dirac points are gapped by impurity scattering. This mirror symmetry breaking by impurity has, however, no effect on the Chern number in a ferromagnetically doped system, as long as the intensity of the random potential is much smaller compared with the Zeeman gap. This is because the Chern number, unlike the mirror Chern number, does not presume any symmetry, as long as the surface is gapped. Weak interactions smaller than the Zeeman gap do not have any effect on the quantized Hall conductance either, because the Chern number is also a good quantum number of an interacting gapped 2D system [40,41].

It is also interesting to discuss other surface terminations besides the (001) surface. On the (110) surface of SnTe, first principles calculations [23] show that there are two Dirac cones centered at two Dirac points that are close to and symmetric about $\bar{X}\,\bar{M}$ along $\bar{\Gamma}\,\bar{X}$ in the surface BZ. The two Dirac points are protected by the $(1\bar{1}0)$ mirror plane and have equal energy due to the (001) mirror plane. A Zeeman field along [110] gaps both Dirac points and results in a QAH phase with Chern number of ± 2. A strain along the $[1\bar{1}1]$ direction breaks both the $(1\bar{1}0)$ and the (001) mirror planes, opening two gaps of opposite signs at the two Dirac points. When both the strain and the Zeeman field are present, a similar discussion shows that the Chern number can be either ± 1 or ± 2. On the (111) surface, there are four Dirac cones centered at $\bar{\Gamma}$ and three $\bar{M}$'s. The three Dirac points at $\bar{M}$ have the same energy due to the threefold rotation symmetry about the [111] axis, while the one at $\bar{\Gamma}$ generically has a different energy. This energy difference among the Dirac points, which has been measured to be $\sim$40 meV in Ref. [27], makes it hard to have a fully gapped surface using an induced Zeeman field, because the Zeeman gap is generically much smaller than 40 meV. Therefore, an insulator with quantized Hall conductance on the (111)-surface is not possible using the current scheme.

The Chern numbers in this system can be measured by conventional four-terminal resistance measurements, as in Refs. [9,10,42], with additional gates to control the Fermi level and the piezoelectric strain.

C. F. and B. A. B. thank A. Yazdani, R. J. Cava, N. P. Ong, A. Alexandradinata, and W.-F. Tsai for helpful discussions. C. F. specially thanks J. Liu and H. Lin for providing useful information on thin-film samples. C. F. is supported by ONR-N00014-11-1-0635. M. J. G. acknowledges support from the AFOSR under Grant No. FA9550-10-1-0459 and the ONR under Grant No. N0014-11-1-0728. B. A. B. was supported by NSF CAREER DMR- 095242, ONR-N00014-11-1-0635, Darpa- N66001-11-1-4110, the David and Lucile Packard Foundation, and MURI-130-6082.

[1] K. v. Klitzing, G. Dorda, and M. Pepper, Phys. Rev. Lett. **45**, 494 (1980).
[2] F. D. M. Haldane, Phys. Rev. Lett. **61**, 2015 (1988).
[3] M. Onoda and N. Nagaosa, Phys. Rev. Lett. **90**, 206601 (2003).
[4] X.-L. Qi, T. L. Hughes, and S.-C. Zhang, Phys. Rev. B **78**, 195424 (2008).
[5] R. Yu, W. Zhang, H.-J. Zhang, S.-C. Zhang, X. Dai, and Z. Fang, Science **329**, 61 (2010).
[6] K. Nomura and N. Nagaosa, Phys. Rev. Lett. **106**, 166802 (2011).
[7] H. Jiang, Z. Qiao, H. Liu, and Q. Niu, Phys. Rev. B **85**, 045445 (2012).
[8] J. Wang, B. Lian, H. Zhang, Y. Xu, and S.-C. Zhang, Phys. Rev. Lett. **111**, 136801 (2013).
[9] C.-Z. Chang *et al.*, Science **340**, 167 (2013).
[10] J. Zhang*et al.*, Science **339**, 1582 (2013).
[11] M. Z. Hasan and C. L. Kane, Rev. Mod. Phys. **82**, 3045 (2010).
[12] X. L. Qi and S. C. Zhang, Rev. Mod. Phys. **83**, 1057 (2011).
[13] A. B. Bernevig and T. L. Hughes, *Topological Insulators and Topological Superconductors* (Princeton University Press, Princeton, NJ, 2013).
[14] S. Cho, N. P. Butch, J. Paglione, and M. S. Fuhrer, Nano Lett. **11**, 1925 (2011).
[15] S. Cho, B. Dellabetta, A. Yang, J. Schneeloch, Z. Xu, T. Valla, G. Gu, M. J. Gilbert, and N. Mason, Nat. Commun. **4**, 1689 (2013).
[16] L. Fu, Phys. Rev. Lett. **106**, 106802 (2011).
[17] T. Hsieh, H. Lin, J. Liu, W. Duan, A. Bansil, and L. Fu, Nat. Commun. **3**, 982 (2012).
[18] S.-Y. Xu*et al.*, Nat. Commun. **3**, 1192 (2012).
[19] P. Dziawa *et al.*, Nat. Mater. **11**, 1023 (2012).
[20] Y. Tanaka, Z. Ren, T. Sato, K. Nakayama, S. Souma, T. Takahashi, K. Segawa, and Y. Ando, Nat. Phys. **8**, 800 (2012).
[21] C. Fang, M. J. Gilbert, S.-Y. Xu, B. A. Bernevig, and M. Z. Hasan, Phys. Rev. B **88**, 125141 (2013).
[22] Y. J. Wang, W.-F. Tsai, H. Lin, S.-Y. Xu, M. Neupane, M. Hasan, and A. Bansil, Phys. Rev. B **87**, 235317 (2013).
[23] J. Liu, W. Duan, and L. Fu, Phys. Rev. B **88**, 241303 (2013).
[24] Y. Okada*et al.*, arXiv:1305.2823.
[25] A. J. Elleman and H. Wilman, Proc. Phys. Soc. London **61**, 164 (1948).
[26] E. G. Bylander, Mater. Sci. Eng. **1**, 190 (1966).
[27] A. A. Taskin, S. Sasaki, K. Segawa, and Y. Ando, arXiv:1305.2470.
[28] M. P. Mathur, D. W. Deis, C. K. Jones, A. Patterson, W. J. Carr Jr., and R. C. Miller, J. Appl. Phys. **41**, 1005 (1970).
[29] M. Inoue, H. Yagi, K. Ishii, and T. Tatsukawa, J. Low Temp. Phys. **23**, 785 (1976).
[30] M. D. Nielsen, E. M. Levin, C. M. Jaworski, K. Schmidt-Rohr, and J. P. Heremans, Phys. Rev. B **85**, 045210 (2012).
[31] See Supplemental Material at http://link.aps.org/supplemental/10.1103/PhysRevLett.112.046801 for (i) The derivation of $h_1(\mathbf{q})$ using the little group at D_i; (ii) how the four Dirac cones are related by C_4 symmetry; (iii) the calculation of the Chern number of the top/bottom surface; (iv) the diagonalization of the surface Hamiltonian in the presence of hybridization and (v) a detailed derivation of Table I.
[32] R. B. Schoolar and J. N. Zemel, J. Appl. Phys. **35**, 1848 (1964).
[33] J. N. Zemel, J. D. Jensen, and R. B. Schoolar, Phys. Rev. **140**, A330 (1965).
[34] M. Shayegan, K. Karrai, Y. P. Shkolnikov, K. Vakili, E. P. D. Poortere, and S. Manus, Appl. Phys. Lett. **83**, 5235 (2003).
[35] D. Berlincourt and H. Jaffe, Phys. Rev. **111**, 143 (1958).
[36] J. Bierly, L. Muldawer, and O. Beckman, Acta Metall. **11**, 447 (1963).
[37] P. B. Littlewood *et al.*, Phys. Rev. Lett. **105**, 086404 (2010).
[38] H. Lin (private communications).
[39] J. Liu, T. H. Hsieh, W. Duan, J. Moodera, and L. Fu, in *APS March Meeting* (2013).
[40] X. L. Qi, Y. S. Wu, and S. C. Zhang, Phys. Rev. B **74**, 045125 (2006).
[41] M. Kohmoto, Ann. Phys. (N. Y) **160**, 343 (1985).
[42] M. König, S. Wiedmann, C. Brüne, A. Roth, H. Buhmann, L. Molenkamp, X.-L. Qi, and S.-C. Zhang, Science **318**, 766 (2007).